Electronic Supplementary Material (ESI) for Physical Chemistry Chemical Physics.

Supporting Information

Boron based layered electrode materials for metal-ion batteries

Kuan-Rong Hao[a, b], Qing-Bo Yan[b*], Gang Su[a, c*]

[a]School of Physical Sciences, University of Chinese Academy of Sciences, Beijing 100049, China.

[b]Center of Materials Science and Optoelectronics Engineering, College of Materials Science and Optoelectronic Technology, University of Chinese Academy of Sciences, Beijing 100049, China.

[c]Kavli Institute for Theoretical Sciences, and CAS Center of Excellence in Topological Quantum Computation, University of Chinese Academy of Sciences, Beijing 100190, China

*Correspondence authors. Email: yan@ucas.ac.cn; gsu@ucas.ac.cn

Table of Contents

1. The geometrical structures of various lithium borides

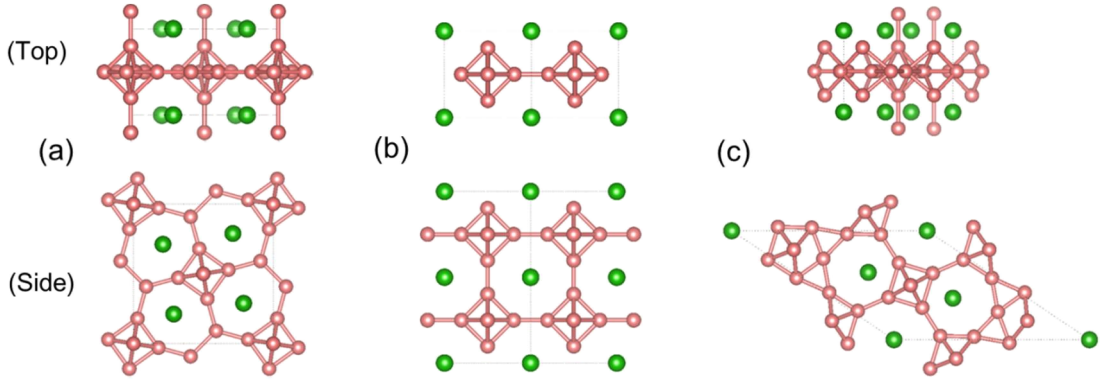

Figure S1. Top and side views of the geometric structures of lithium borides (a) MB_4; (b) MB_6; (c) M_3B_{20} (M = Li, Na), respectively;

We perform a systematical investigation on various boron based layered compounds. As shown in Fig. S1, because of the structure features formed by boron octahedron and boron rings, typical metal borides including MB_4, MB_6 and M_3B_{20} (M = Li, Na) have been considered. However, due to the dynamic instability of LiB_4, LiB_6 and Li_3B_{20} and high energy barrier of Na ion in NaB_4, NaB_6, Na_3B_{20}, they are restricted to the metal electrode materials.

2. The migration and phonon dispersion curves of LiB_4

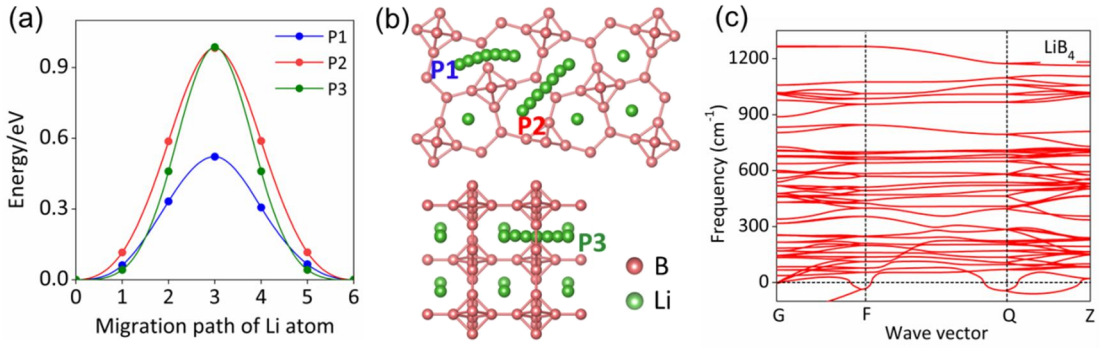

Figure S2. The diffusion energy barriers (a), three possible migration paths (b) of Li ions along the P1, P2, P3 and (c) phonon dispersion curve of LiB_4.

Here, we show some results of LiB_4 as an example, as shown in Fig. S2 (a) and (b), with the diffusion path P1 indicated. It can be seen that just 0.52 eV energy barrier is needed to be overcome for Li ions, which is lower than that in $LiAlB_4$. The barrier values of 0.98 eV and 0.99 eV for P2 and P3 paths were obtained, which are obviously higher than that along the P1 path. In addition, the phonon dispersion illustrates apparent imaginary modes. Thus, this compound fails in serving as electable electrode material.

3. Phonon dispersions of $Na/MgAlB_4$, $Na/MgGaB_4$

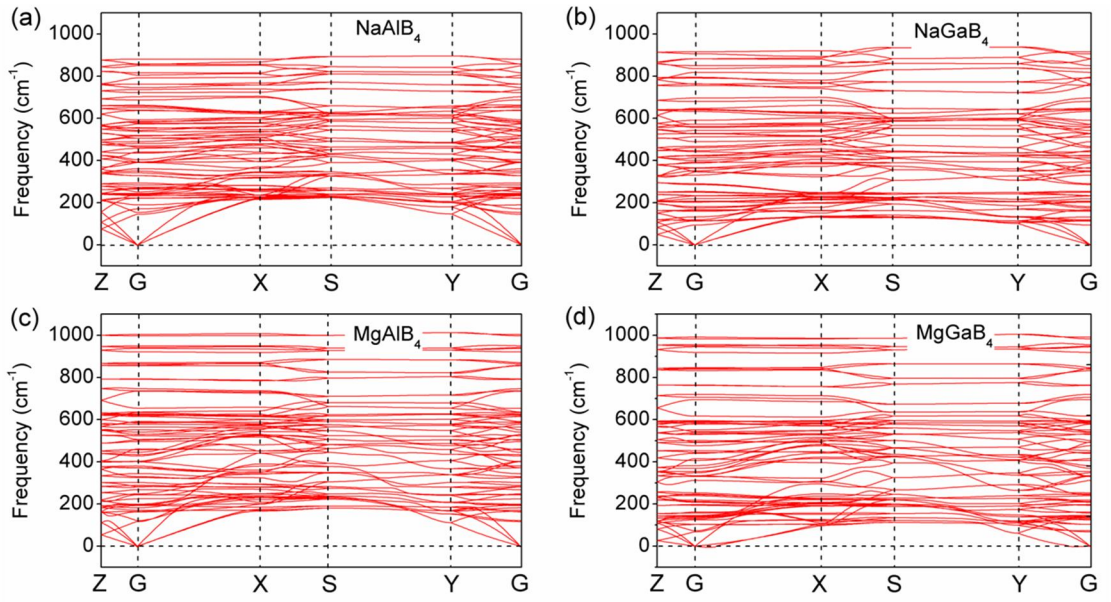

Figure S3. The calculated phonon dispersions for (a) $NaAlB_4$, (b) $NaGaB_4$, (c) $MgAlB_4$ and (d) $MgGaB_4$, respectively.

In order to confirm the dynamic stability, firstly, the phonon dispersions are calculated for the structures of $Na/MgAlB_4$, $Na/MgGaB_4$, as presented in Fig. S3. No imaginary phonon modes are found, indicating that they all are dynamically stable.

4. The electron density of states of $Na/MgAlB_4$ and $Na/MgGaB_4$

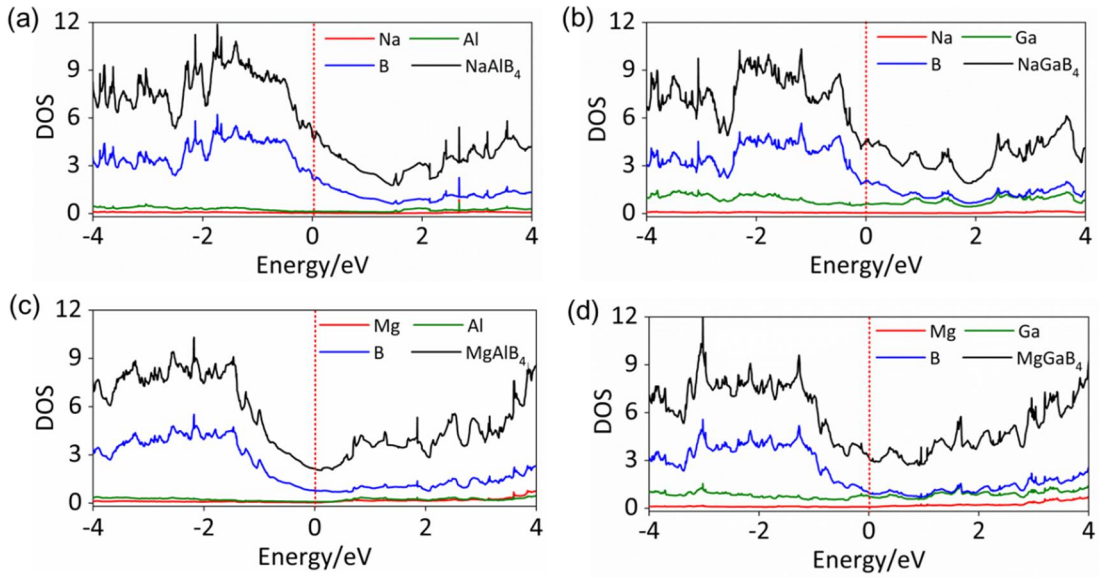

Figure S4. The total and projected electron density of states (DOS) of (a) $NaAlB_4$, (b) $NaGaB_4$, (c) $MgAlB_4$ and (d) $MgGaB_4$, respectively.

As shown in Fig. S4, the calculated electron structures illustrate that they are metallic with electronic states existing on the Fermi level. The curves of DOS show that the contributions of the *s* electrons of Na and Mg atoms to the density of states especially valence states are very small and the boron electron states are prominent. Similarly, a comparison between $MAlB_4$ and $MGaB_4$ (M = Li, Na) also reveals that the DOS of Ga atoms are more dominant than that of Al atoms.

5. The electron band structures of M_xXB_4 (*M* = Li, Na, Mg; *X* = Al, Ga)

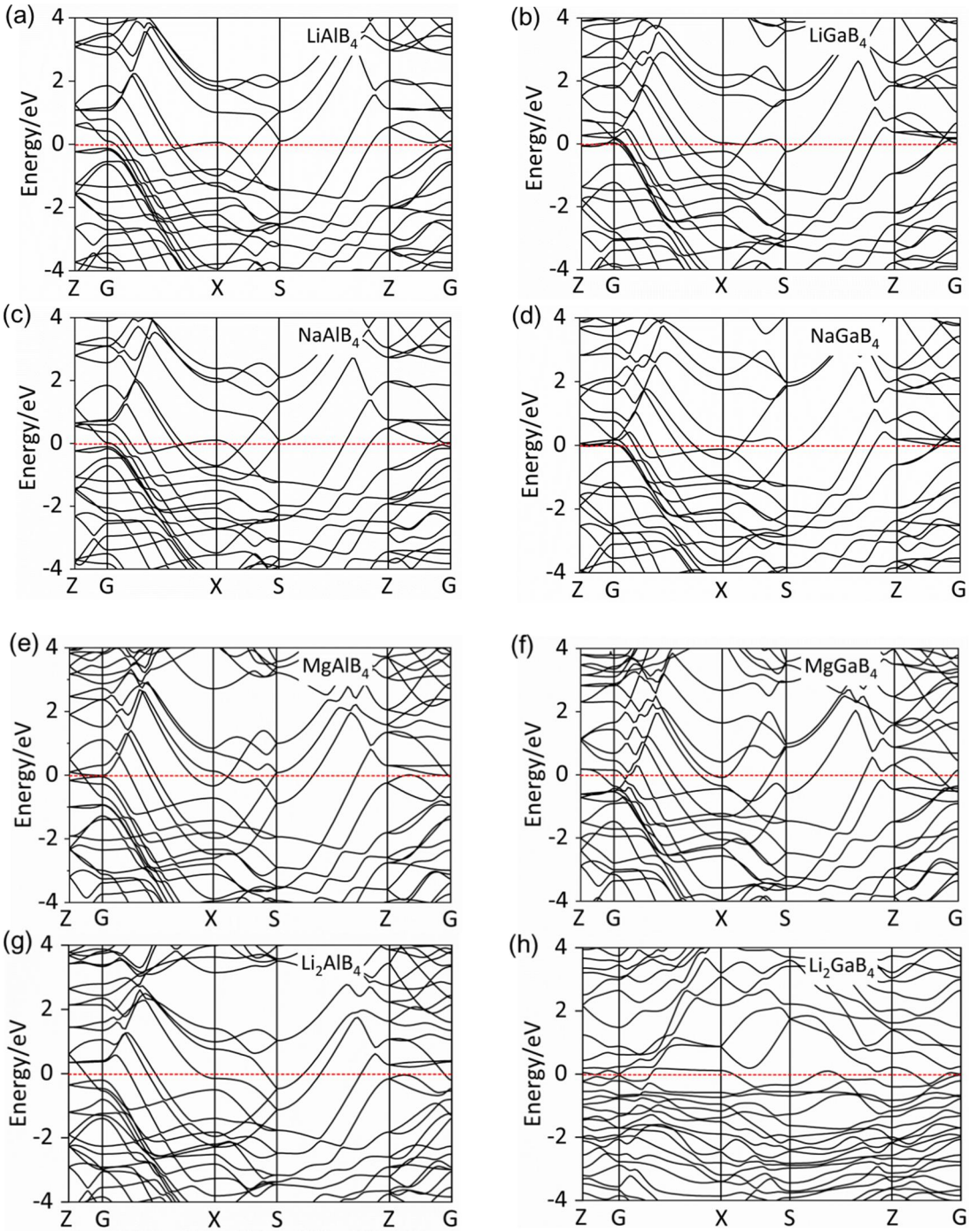

Figure S5. The electron band structures of (a) $LiAlB_4$, (b) $LiGaB_4$, (c) $NaAlB_4$, (d) $NaGaB_4$, (e) $MgAlB_4$, (f) $MgGaB_4$, (g) Li_2AlB_4 and (h) Li_2GaB_4, respectively.

6. The volume change of Li_xAlB_4

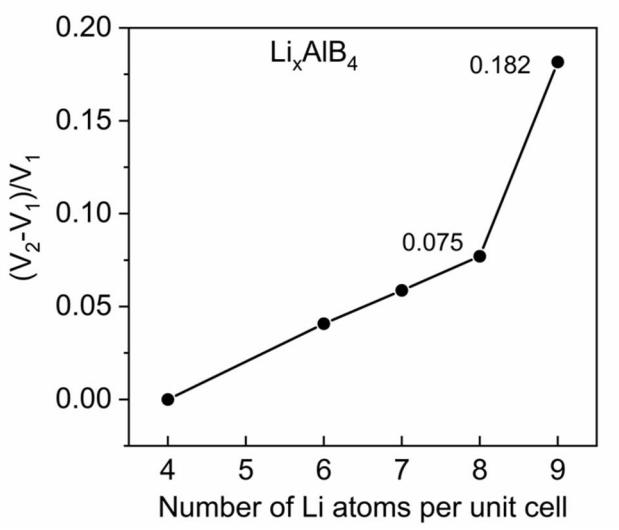

Figure S6. The volume change rate of Li_xAlB_4.

In order to further illustrate the structural stability of Li_xAlB_4 during the process of lithium ions de-intercalation, the volume expansion was measured by $\eta = (V_2-V_1)/V_1$ (V_1 is the volume of $Li_4X_4B_{16}$, V_2 is the volume of $Li_xX_4B_{16}$(x = 6, 8, 7, 9)). For $Li_xAl_4B_{16}$(x = 4, 6, 7, 8), the structure remains intact andηgrows linearly as shown in Fig. S6, and the value of η estimated as 7.5% for $Li_8Al_4B_{16}$ goes well with the volume expansion tolerance. While x = 9, the structure is obviously distorted and η reaches to 18.2%, which may goes beyond the lattice distortion and expansion tolerance and may be inappropriate for practical applications.

7. The calculated elastic constants of M_xXB_4 (M = Li, Na, Mg; X = Al, Ga)

	$LiAlB_4$	$NaAlB_4$	$MgAlB_4$	$LiGaB_4$	$NaGaB_4$	$MgGaB_4$	Li_2AlB_4	Li_2GaB_4
C_{11}	271.25	262.22	380.99	283.46	257.52	246.86	339.29	85.026
C_{22}	372.67	358.82	431.89	348.04	335.40	386.31	284.78	297.69
C_{33}	363.11	375.84	421.47	343.99	354.48	369.79	358.83	259.62
C_{44}	46.92	71.32	38.59	25.58	46.26	5.45	188.58	39.3
C_{55}	184.41	176.63	200.78	163.77	163.11	167.13	28.51	131.92
C_{66}	45.24	68.19	42.96	20.31	414.54	11.50	15.83	53.27
C_{12}	38.51	41.15	1.37	37.15	39.04	35.49	151.25	43.98
C_{13}	36.21	41.11	7.40	35.44	43.65	44.89	1.05	60.30
C_{23}	87.75	65.80	126.03	93.97	74.21	114.47	-19.54	49.82

Table S1. The calculated elastic constants Cij (in GPa) for orthorhombic crystal M_xXB_4 (M = Li, Na, Mg; X = Al, Ga).

As we all know, for a given orthorhombic crystal, there are nine independent elastic constants (C_{11}, C_{22}, C_{33}, C_{44}, C_{55}, C_{66}, C_{12}, C_{13}, C_{23}), which should satisfy the Born stability criteria for mechanical stability as flowing:

$C_{ii} > 0$ (i = 1, 2, 3, 4, 5, 6);

$C_{11} + C_{22} + C_{33} + 2(C_{12} + C_{13} + C_{23}) > 0$;

$C_{11} + C_{22} - 2C_{12} > 0$; $C_{11} + C_{33} - 2C_{13} > 0$; $C_{22} + C_{33} - 2C_{23} > 0$;

The calculated elastic constants for M_xXB_4 (M = Li, Na, Mg; X = Al, Ga) are listed in Table S1, which shows that all of these compounds satisfy all above mechanical stability conditions. Therefore, they are mechanically stable.

8. The density states of phonon for $LiAl/GaB_4$ and Li_2Al/GaB_4

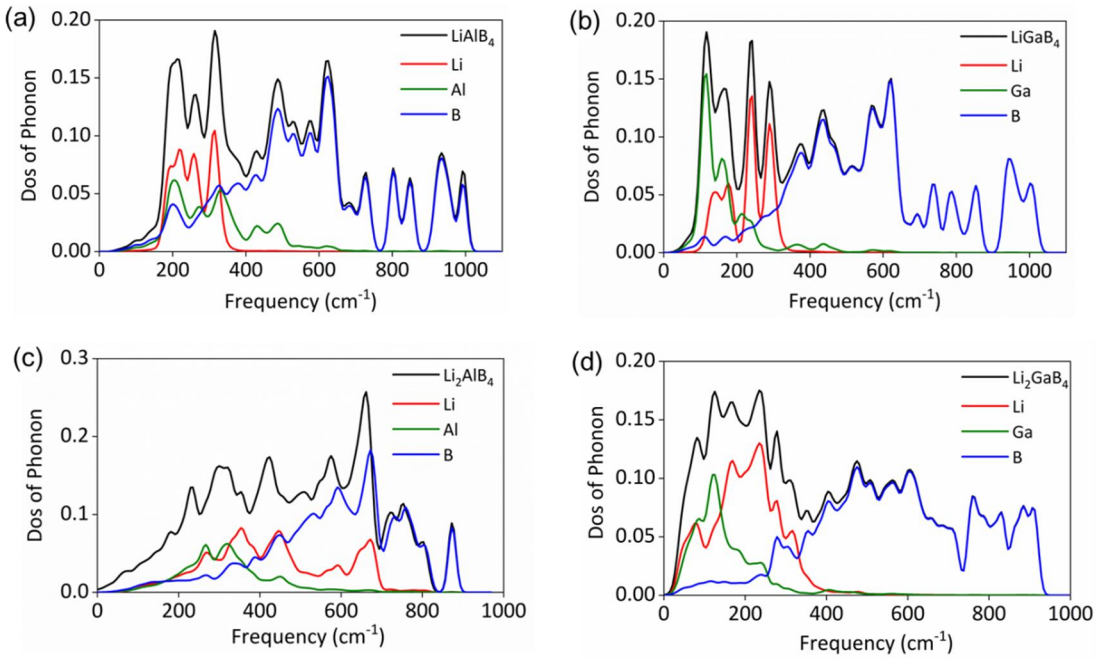

Figure S7. The total and projected phonon density of states for (a) $LiAlB_4$, (b) $LiGaB_4$, (c) Li_2AlB_4 and (d) Li_2GaB_4, respectively.

As shown in Fig. S7, the phonon density states of Ga atoms mainly contribute in the low-frequency region and are larger than that of Al atoms. From Fig. S7 (a) (b) and (d), it is obviously seen that the primary contributions of phonon density of states in the low-frequency region come from Li and Al/Ga atoms, and the high frequency (>400 cm^{-1}) is mainly from the boron atoms. In Li_2AlB_4, the distribution of DOS of phonon for Li atoms stretches across the range of 200 cm^{-1} - 700 cm^{-1} due to its structure.